A *Suzaku* View of Cyclotron Line Sources and Candidates

K. Pottschmidt[*,†], S. Suchy[**], E. Rivers[**], R. E. Rothschild[**], D. M. Marcu[*,†], L. Barragán[‡,§], M. Kühnel[‡,§], F. Fürst[‡,§], F. Schwarm[‡,§], I. Kreykenbohm[‡,§], J. Wilms[‡,§], G. Schönherr[¶], I. Caballero[‖], A. Camero-Arranz[††,‡‡], A. Bodaghee[§§], V. Doroshenko[¶¶], D. Klochkov[¶¶], A. Santangelo[¶¶], R. Staubert[¶¶], P. Kretschmar[***], C. Wilson-Hodge[‡‡], M. H. Finger[††,‡‡] and Y. Terada[†††]

[*]*CRESST and NASA Goddard Space Flight Center, Astrophysics Science Division, Code 661, Greenbelt, MD 20771, USA*
[†]*Center for Space Science and Technology, University of Maryland Baltimore County, 1000 Hilltop Circle, Baltimore, MD 21250, USA*
[**]*University of California, San Diego, Center for Astrophysics and Space Sciences, 9500 Gilman Dr., La Jolla, CA 92093-0424, USA*
[‡]*Dr. Karl Remeis-Observatory, Sternwartstr. 7, 96049 Bamberg, Germany*
[§]*Erlangen Centre for Astroparticle Physics, University of Erlangen-Nuremberg, Erwin-Rommel-Strasse 1, 91058 Erlangen, Germany*
[¶]*Astrophysikalisches Institut Potsdam, 14482 Potsdam, Germany*
[‖]*CEA SAclay, DSM/IRFU/SAp –UMR AIM (7158) CNRS/CEA/Univ. P. Diderot –F-91191, France*
[††]*Universities Space Research Association, Huntsville, AL 35806, USA*
[‡‡]*Space Science Office, VP62, NASA/Marshall Space Flight Center, Hunstville, AL 35812, USA*
[§§]*Space Sciences Laboratory, 7 Gauss Way, University of California, Berkeley, CA 94720, USA*
[¶¶]*Institut für Astronomie und Astrophysik Astronomie, Sand 1, 72076 Tübingen, Germany*
[***]*ESA-European Space Astronomy Centre, 28691 Villanueva de la Cañada, Madrid, Spain*
[†††]*Graduate School of Science and Engineering, Saitama University, 255 Simo-Ohkubo, Sakura-ku, Saitama City, Saitama 338-8570, Japan*

Abstract. Seventeen accreting neutron star pulsars, mostly high mass X-ray binaries with half of them Be-type transients, are known to exhibit Cyclotron Resonance Scattering Features (CRSFs) in their X-ray spectra, with characteristic line energies from 10 to 60 keV. To date about two thirds of them, plus a few similar systems without known CRSFs, have been observed with *Suzaku*. We present an overview of results from these observations, including the discovery of a CRSF in the transient 1A 1118−61 and pulse phase resolved spectroscopy of GX 301−2. These observations allow for the determination of cyclotron line parameters to an unprecedented degree of accuracy within a moderate amount of observing time. This is important since these parameters vary – e.g., with orbital phase, pulse phase, or luminosity – depending on the geometry of the magnetic field of the pulsar and the properties of the accretion column at the magnetic poles. We briefly introduce a spectral model for CRSFs that is currently being developed and that for the first time is based on these physical properties. In addition to cyclotron line measurements, selected highlights from the *Suzaku* analyses include dip and flare studies, e.g., of 4U 1907+09 and Vela X-1, which show clumpy wind effects (like partial absorption and/or a decrease in the mass accretion rate supplied by the wind) and may also display magnetospheric gating effects.

Keywords: pulsars: individual (1A 1118−61, GX 301−2, 4U 1907+09, Vela X-1) — stars: magnetic fields — stars: neutron — X-rays: binaries
PACS: 97.80.Jp, 98.70.Qy, 97.60.Gb

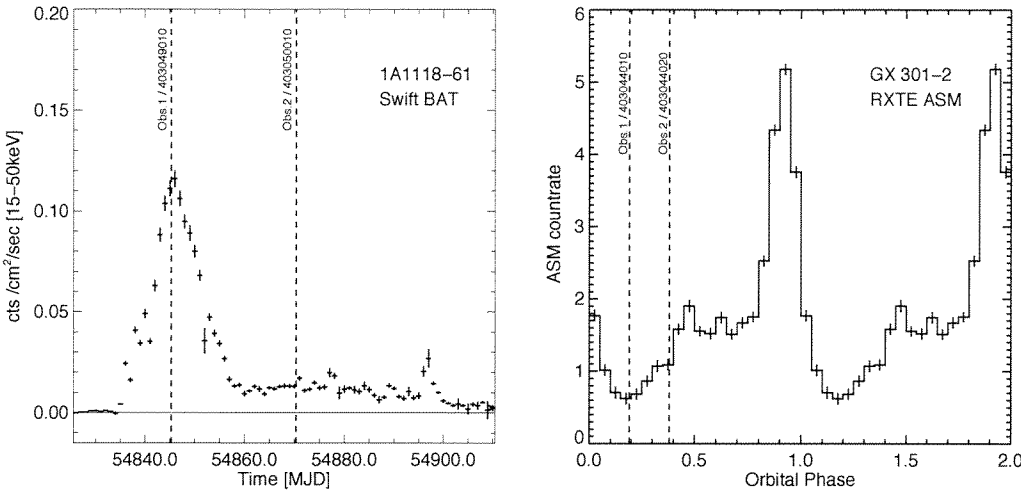

FIGURE 1. Left: *Swift*-BAT 15–50 keV light curve of the transient accreting pulsar 1A 1118−61 showing the 2009 outburst of the source. Vertical lines indicate the times of the January 15, 2009, and January 28, 2009, *Suzaku* pointings (exposures of ∼50 ks and ∼30 ks, respectively). **Right:** *RXTE*-ASM 1–12 keV orbital profile of the persistent accreting pulsar GX 301−2. Vertical lines indicate the orbital phases of the August 25, 2008, and January 5, 2009, *Suzaku* pointings (exposures of ∼10 ks and ∼60 ks, respectively). After [1] and [2].

1. INTRODUCTION

Accreting X-ray pulsars were first discovered in the 1970s with the detection of the 4.8 s pulsation of Cen X-3 [3]. In these sources the compact object is a highly magnetized neutron star leading to accretion of material along the magnetic field lines and the formation of X-ray emitting accretion columns above the neutron star's magnetic poles. These sources can also show absorption-line-like scattering features in their X-ray spectra at multiples of $E_{\rm cycl} \sim 11.6\,{\rm keV} \times B[10^{12}\,{\rm G}]$ since for such strong magnetic fields electron energies are quantized. Observations of sources with cyclotron resonant scattering features (CRSF, cyclotron lines) provide us with the most direct information for studying strong magnetic fields. *Suzaku* is especially well suited to find/study cyclotron lines due to its broadband X-ray coverage at high sensitivity with comparatively low background. With O- or B-type donor stars most CRSF sources are high mass X-ray binaries (exceptions: Her X-1, 4U 1626−67). Those in the first block of Table 1 (plus persistent X Per and some of the potential CRSF candidates in the third block) are Be type X-ray binaries which are generally transient [4]. They typically have eccentric orbits and their X-ray activity is triggered when the neutron star crosses a disk of material that surrounds the equator of the Be/Oe star. Between outbursts they can show years long quiescence periods. While the CRSF sources listed in the second block of Table 1 are persistent X-ray emitters they are very variable on all observed time scales, reflecting stellar wind, magnetosphere (see, e.g., [5, 6] for Vela X-1), or accretion disk structure (see, e.g., [7] for Her X-1). Fig. 1 shows examples of typical long term variability for a transient and a persistent source. For recent reviews on accreting pulsars see [8] and [9].

TABLE 1. Properties of a sample of accreting pulsars. 1–9: All known transient CRSF sources. 10–17: All known persistent CRSF sources. 18–27: Selected potential CRSF candidates. All sources with names not printed in italics have been observed with *Suzaku* ($1\times - 4\times$) at the time of writing. The pulse period $P_{\rm pulse}$ usually varies with luminosity and time. The same is often true for the cyclotron line energies $E_{\rm cycl}$ which can also vary with pulse phase. Here we quote representative values from the overall literature. ***Suzaku* results for sources with names in bold face are discussed in this work.**

	Source Name	**CRSF Energies $E_{\rm cycl}$ [keV]**	**Pulse Period $P_{\rm pulse}$ [s]**	**Orbital Period $P_{\rm orbit}$ [d]**	**Type**	***Suzaku* analysis reference**
1	*Swift J1626.6−5156*	10	15	132.9	T, Be	
2	4U 0115+63	14, 24, 36 48, 62	3.6	24.31	T, B0.2 Ve	work in progress
3	*V 0332+53*	27, 51, 74	4.37	34.25	T, O8.5 Ve	
4	*Cep X-4*	28	66.25	>23	T, B1.5 Ve	
5	*MXB 0656−072*	33	160	?	T, O9.7 Ve	
6	XTE J1946+274	36	15.8	169.2	T, B0-1 V-IVe	work in progress
7	1A 0535+26*	45, 100	105	110.58	T, O9.7 IIe	[10] [11] [12]
8	GX 304−1†	54	272	?	T, B2 Vne	[13]
9	**1A 1118−616**	55, 112?	408	24	T, O9.5 IV-Ve	[1]
10	**4U 1907+09**	19, 40	438	8.38	P, B2 III–IV	[14]
11	*4U 1538−52*	20	530	3.73	P, B0 I	
12	**Vela X-1**	25, 53	283	8.96	P, B0.5 Ib	[15]
13	*X Per*	29	837	250.3	P, B0 III–Ve	
14	Cen X-3	30	4.8	2.09	P, O6.5 II	[16]
15	**GX 301−2**	37	690	41.5	P, B1.2 Ia	[2]
16	4U 1626−67	37	7.66	0.028	P, LMXB	[17]
17	Her X-1	39	1.24	1.7	P, A9-B	[18] [19]
18	EXO 2030+375	11? 63?	42	46.0	T, B0 Ve	work in progress
19	GRO J1008−57	88?	93.7	249.5	T, B0e	[20] [21]
20	*LS V +44 17*		202	?	T, B0.2 Ve	
21	*GS 1843+00*	20?	29.5	?	T, B0-2 IV-Ve	
22	XTE J1739−302**		?	51.47	T, O8 Iab	[22]
23	*OAO 1657−415*	36?	37.7	10.4	P, B0-B6 Ia-Iab	
24	4U 1700−377	37?	?	3.4	P, O6.5 Iaf+	work in progress
25	LMC X-4	100?	13.5	1.41	P, O7 IV	[23]
26	4U 1909+07		604	4.4	P, OB	work in progress
27	IGR 16318−4848		?	?	P, sgB[e]	[24]

* Caballero et al., see elsewhere in these proceedings

† Yamamoto et al., see elsewhere in these proceedings

** Bodaghee et al., see elsewhere in these proceedings

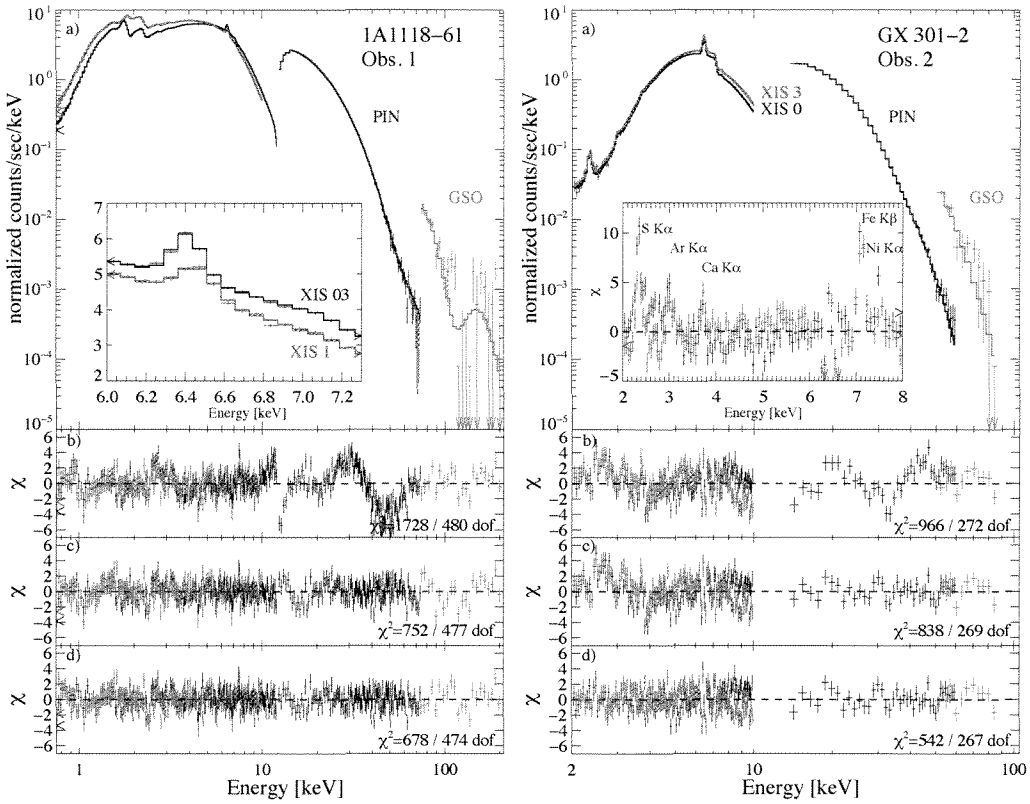

FIGURE 2. Left: The main panel shows the *Suzaku* broad band spectrum and best fit of the brighter 1A 1118−61 observation with an inset highlighting the iron line region. Residuals are shown including no CRSF (a), including one CRSF at 58 keV (b), and including a second CRSF at 112 keV (c, best fit). **Right:**. The main panel shows the *Suzaku* broad band spectrum and best fit of the brighter GX 301−2 observation with an inset highlighting the emission line residuals from neutral material which remain after modeling Fe Kα. (The back illuminated XIS1 was modeled separately here, with consistent results.) Residuals are shown including no CRSF and not accounting for partial covering absorption (a), including a CRSF at 35 keV (b), and also accounting for partial covering (c, best fit). After [1] and [2].

2. *SUZAKU* OBSERVATIONS

2.1. Discovery of a CRSF in 1A 1118+61

After only two previously observed outbursts (1974, 1992) the Be X-ray binary 1A 1118−61 went into outburst in January 2009 and was observed with *Suzaku* at the $\sim$ 500 mCrab outburst peak and two weeks later at the end of the main outburst (Fig. 1, left). Together with quasi-simultaneous *RXTE* observations [6] these observations enabled the discovery of a $\sim$ 55 keV cyclotron line in this source [1] (Fig. 2, left). *RXTE*, *Swift*-BAT, and *Suzaku* also co-discovered another cyclotron line, namely the $\sim$ 54 keV feature in GX 304−1 [25, 13]. Furthermore there are indications that the line in 1A 1118−61 may be luminosity dependent. With $E_{\rm cycl}$ values of $58.2^{+0.8}_{-0.4}$ keV and

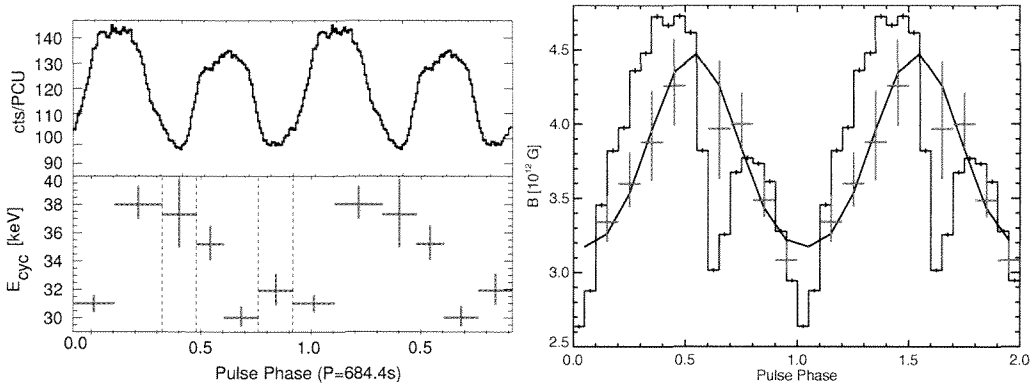

FIGURE 3. **Left:** Results from a $\sim$ 200 ks *RXTE* observation of GX 301−2, after [27]. The upper panel shows the double peaked pulse profile in the 19-60 keV energy band (twice for clarity). The lower panel shows that the cyclotron line energy varies by ~20% over one cycle. Vertical lines indicate pulse profile minima. **Right:** Results from a $\sim$ 60 ks *Suzaku* observation of GX 301−2 ("obs 2" from Fig. 1 and Fig. 2), after [2]. The red data points confirm the $E_{\rm cycl}$ variations, translated into directly $E_{\rm cycl}$ proportional B-field variations. The black curve shows the best fit magnetic dipole model described in the text. The blue histogram indicates the 1–10 keV pulse profile (arbitrary normalization).

$47.4^{+3.2}_{-2.3}$ keV for the flare and decline observation, respectively, the source would show a positive L-$E_{\rm cycl}$ correlation like Her X-1. Negative or no correlations have recently been observed for other CRSF sources [8]. A possible explanation for the existence of positive and negative correlations is the different state of the accretion column in the sub- and super-Eddington regimes [26].

2.2. Pulse Phase Resolved Analysis of GX 301−2

The persistent accreting pulsar GX 301−2 was observed twice with *Suzaku*, during less bright and less well studied orbital phases outside of the pre-periastron flare (Fig. 1, right). These observations allowed for a detailed study of the highly absorbed phase averaged spectrum, including several fluorescence emission lines and the well known 37 keV CRSF (Fig. 2, right) as well as of pulse phase resolved spectra for the second, longer observation [2]. Strong variations of the cyclotron line energy $E_{\rm cycl}$ with pulse phase had been discovered in an *RXTE* observation dominated by the comparatively bright pre-periastron flare [27] (Fig. 3, left, lower panel). Several other CRSF sources are known to show similarly strong variations (see, e.g., [28] and references given by [27, 1]). Even though the *Suzaku* observation does not cover the bright pre-periastron flare a clear pattern for the $E_{\rm cycl}$ variations emerges within a comparatively modest exposure time (Fig. 3, right). Assuming a simple magnetic dipole the B-field projected onto the line of sight can be calculated for each phase bin, depending on a set of geometric angles. This leads to four symmetrically equivalent best fit solutions. Model constraints derived using the observed ratio of the width of the cyclotron line and $E_{\rm cycl}$ favor a solution wherein the spin axis is tilted by 15° with respect to the line of sight [2].

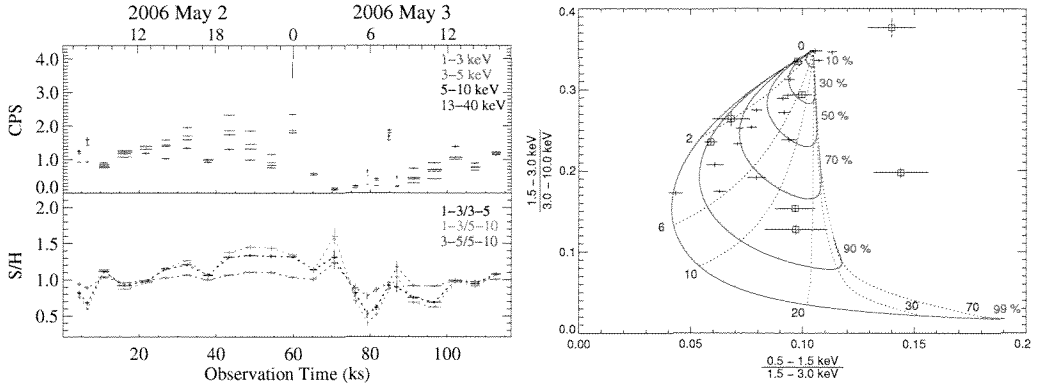

FIGURE 4. Left: Energy-resolved, background-subtracted light curves (upper panel), and softness ratios (lower panel) from XIS0 for the 2006 *Suzaku* observation of 4U 1907+09. **Right:** Color-color diagram from added XIS0 and XIS3 data for the same observation. Boxed data points correspond to the deep dip in the light curve between 60 ks and 100 ks. Grid lines indicate hardness values from spectral models obtained by increasing the covering fraction at constant $N_{\rm H}$ (blue) or vice versa (red) compared to the best fit spectral model for times without additional partial covering absorption or flaring. From [14].

2.3. Dips & Flares: Stellar Wind Structure

2.3.1. 4U 1907+09

The ~20 mCrab accreting pulsar 4U 1907+09 is characterized by a highly variable persistent flux as well, but in this case the dips and flares do not seem to be related to the orbital phase [29, 14]. *Suzaku* observed the source on May 2–3, 2006, and April 19–20, 2007, for respectively ~60 ks and ~ 80 ks. Both observations display dips and flares (Fig. 4, left, shows the 2006 case). It had been noted before that the dipping might not be due to absorption but due to cessation of accretion [29]. Using color-color diagrams [14] found that while some of the flux and hardness variability is consistent with absorption there are indeed events where this is not the case, i.e., for the deep dip in the 2006 dataset (Fig. 4, right). They conclude that the overall behavior is consistent with a clumpy wind.

2.3.2. Vela X-1

Even more extreme flux variability, so called off states and giant flares – both with flux changes of up to a factor of ~20 – have been discovered with *INTEGRAL* for Vela X-1 [30]. During the off states no pulsations were observed with *INTEGRAL*. *Suzaku* detected three off-sates during a 100 ks observation on June 17–18, 2008, lasting up to 3.2 ks [6]. Due to *Suzaku's* sensitivity pulsations could still be detected. [6] suggest that while the off states might be triggered by stellar wind inhomogeneities they are consistent with gated accretion where Kelvin-Helmholz instabilities allow for some matter to leak into the magnetosphere.

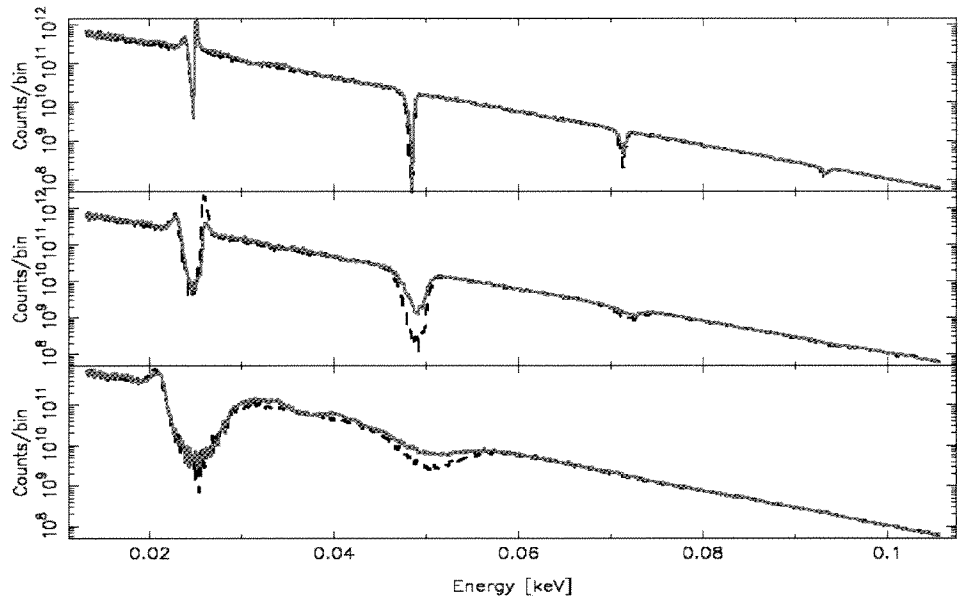

FIGURE 5. Comparison of spectra resulting from the previous (black) and current (red) version of the MC code for simulating physical CRSFs, for three different photon incident angles. From [31]. The input X-ray continuum spectrum is an empirical one (a power law with a Fermi-Dirac cutoff, characterized by $E_{\rm fold} = 10$ keV and $E_{\rm cut} = 12$ keV). The lines, however, are produced in a cylindrical accretion column with a magnetic field of $B/B_{\rm crit} = 0.05$ and an electron plasma temperature and optical depth of $kT_{\rm e} = 3$ keV and $\tau_{\rm es} = 10^{-3}$, respectively. Note that $B_{\rm crit} = m_{\rm e}^2 c^3/e\hbar = 4.414 \times 10^{13}$ G.

3. A PHYSICALLY MOTIVATED CRSF MODEL

Currently empirical models are used to describe cyclotron line features, parametrized, e.g., as absorption with a Gaussian optical depth profile or by a Lorentzian profile (`gabs` and `cyclabs` in `xspec`, respectively). Work has been going on since the 1990s to describe CRSFs in terms of physical parameters like the temperature $kT_{\rm e}$ and optical depth $\tau_{\rm es}$ of the electron plasma in the line forming region, as well as the B-field strength and the accretion geometry [32, 33]. This endeavor reached a recent point of culmination with the implementation of a Monte Carlo (MC) code describing the scattering process, the calculation of a grid of Green's functions which can be used to apply the process to any continuum spectrum, and the development of the `xspec` model `cyclomc` for this task by [34]. First `cyclomc` applications to observed X-ray spectra, e.g., of V 0332+53, resulted in generally acceptable fits and parameter values, with the caveat of stronger emission wings than observed and different relative line depths than expected [34]. With a correction of the scattering cross sections in the most recent iteration of the MC code by [31] this has been resolved. Fig. 5 shows a comparison of CRSFs calculated with the two MC versions for three different photon incident angles with respect to the magnetic field in a cylindrical accretion column. The team is currently in the process of calculating a new grid of Green's functions to be used with `cyclomc`.

4. SUMMARY AND CONCLUSIONS

So far *Suzaku* has observed eleven of the seventeen cyclotron line sources at least once. Two were identified as CRSF sources for the first time (1A 1118−61, GX 304−1). Detailed phase resolved studies can be performed that allow us to constrain the B-field geometry (e.g., GX 301-2). The important $E_{\rm cycl} - L$ relationship can be studied (e.g., 1A 1118−61, 1A 0535+26), potentially with much better time resolution than before (future monitoring observations are desirable). Detailed studies of the mass transfer process (stellar wind, magnetosphere) can be performed as well (e.g., 4U 1907+09, Vela X-1, Cen X-3). Future work is foreseen to include a comparative study of the *Suzaku* sample applying the new `cyclomc` line model.

Acknowledgments: We thank the *Suzaku* team for their help in executing these observations, especially for the excellent timing of the 1A 1118−61 ToO (Fig. 1, left) and the eclipse-to-eclipse Cen X-3 observation (not discussed here due to space limitations).

REFERENCES

1. S. Suchy et al., *Astrophys. J.* **733**, 15 (2011).
2. S. Suchy et al., *Astrophys. J.* (2011), in press.
3. R. Giacconi et al., *Astrophys. J., Lett.* **167**, L67 (1971).
4. P. Reig, *Astrophys. Space. Sci.* **332**, 1 (2011).
5. F. Fürst et al., *Astron. Astrophys.* **519**, A37 (2010).
6. V. Doroshenko et al., *Astron. Astrophys.* **515**, L1 (2010).
7. R. Staubert et al., *Astron. Astrophys.* **494**, 1025 (2009).
8. I. Caballero, and J. Wilms, *Mem. Soc. Astron. Ital.* p. 282 (2011).
9. B. Paul, and S. Naik, *Bull. Astron. Soc. India* (2011), in press (arXiv:1110.4446).
10. Y. Terada et al., *Astrophys. J., Lett.* **648**, L139 (2006).
11. S. Naik et al., *Astrophys. J.* **672**, 516 (2008).
12. I. Caballero et al., *POS (INTEGRAL2010)* p. 63 (2011), in press (arXiv:1107.3417).
13. T. Yamamoto et al., *Publ. Astron. Soc. Jpn.* (2011), in press (arXiv:1102.4232).
14. E. Rivers et al., *Astrophys. J.* **709**, 179 (2010).
15. V. Doroshenko, A. Santangelo, and V. Suleimanov, *Astron. Astrophys.* **529**, 52 (2011).
16. S. Naik, B. Paul, and Z. Ali, *Astrophys. J.* **737**, 79 (2011).
17. A. Camero-Arranz et al., *Astrophys. J.* (2011), in prep.
18. T. Enoto et al., *Publ. Astron. Soc. Jpn.* **60**, 57 (2008).
19. D. Klochkov et al., *Astron. Astrophys.* (2011), in prep.
20. S. Naik et al., *MNRAS* **413**, 241 (2011).
21. M. Kühnel et al., *Astron. Astrophys.* (2011), in prep.
22. A. Bodaghee et al., *Astrophys. J.* **727**, 59 (2011).
23. L.-W. Hung et al., *Astrophys. J.* **720**, 1202 (2010).
24. L. Barragán et al., *Astron. Astrophys.* **508**, 1275 (2009).
25. T. Sakamoto et al., *The Astronomer's Telegram* **2815** (2010).
26. R. Staubert et al., *Astron. Astrophys.* **465**, L25 (2007).
27. I. Kreykenbohm et al., *Astron. Astrophys.* **427**, 975 (2004).
28. S. Suchy et al., *Astrophys. J.* **675**, 1487 (2008).
29. J. J. M. in 't Zand, T. E. Strohmayer, and A. Baykal, *Astrophys. J., Lett.* **479**, L47 (1997).
30. I. Kreykenbohm et al., *Astron. Astrophys.* **492**, 511 (2008).
31. F.-W. Schwarm, *Cyclotron resonant scattering features in the line forming region of highly magnetized neutron stars*, Diploma thesis, Dr. Karl Remeis-Observatory Bamberg, Astronomical Institute of the Friedrich-Alexander-University of Erlangen-Nürnberg (2010), http://www.sternwarte.uni-erlangen.de/new/Arbeiten/2010_09_Schwarm.pdf.
32. A. K. Harding, and J. K. Daugherty, *Astrophys. J.* **374**, 687 (1991).
33. R. A. Araya, and A. K. Harding, *Astrophys. J.* **517**, 334 (1999).
34. G. Schönherr et al., *Astron. Astrophys.* **472**, 353 (2007).